

Mask to reconstruct: Cooperative Semantics Completion for Video-text Retrieval

Han Fang* Zhifei Yang* Xianghao Zang Chao Ban Hao Sun

Abstract

Recently, masked video modeling has been widely explored and significantly improved the model’s understanding ability of visual regions at a local level. However, existing methods usually adopt random masking and follow the same reconstruction paradigm to complete the masked regions, which do not leverage the correlations between cross-modal content. In this paper, we present **M**Ask for **S**emantics **C**OMpleTion (**MASCOT**) based on semantic-based masked modeling. Specifically, after applying attention-based video masking to generate high-informed and low-informed masks, we propose Informed Semantics Completion to recover masked semantics information. The recovery mechanism is achieved by aligning the masked content with the unmasked visual regions and corresponding textual context, which makes the model capture more text-related details at a patch level. Additionally, we shift the emphasis of reconstruction from irrelevant backgrounds to discriminative parts to ignore regions with low-informed masks. Furthermore, we design dual-mask co-learning to incorporate video cues under different masks and learn more aligned video representation. Our **MASCOT** performs state-of-the-art performance on four major text-video retrieval benchmarks, including **MSR-VTT**, **LSMDC**, **ActivityNet**, and **DiDeMo**. Extensive ablation studies demonstrate the effectiveness of the proposed schemes.

1. Introduction

Video-text retrieval is a fundamental task in multi-modal understanding at the video-text level [51]. This process involves searching for a returned video or captions with a given cross-model query and has gained increasing attention from researchers [11, 19, 22, 53, 87]. In the past years, several video-text benchmarks [1, 8, 10, 71, 90] have been proposed to measure performance, which advances the development of video-text retrieval [31, 46, 50, 94].

Traditional video-text retrieval methods typically utilize fixed expert networks [19, 20, 49] to extract spatial, motion, and other features for multimodal fusion [97]. Recently, ad-

vancements in image-text pre-trained models [39, 69] have shown remarkable generalization in video-text understanding [27, 101]. Despite their success, pre-training in the video-text domain requires substantial resources for collecting large amounts of annotated video-text pairs [22]. Consequently, there is a growing interest in transferring knowledge from pre-trained vision-language models to video-text retrieval tasks [53, 54, 99]. Several temporal modeling methods [46, 50] have been proposed for integration with CLIP [69] to enhance global video representation [2, 22] for alignment. However, the neglect of local semantic extraction has hindered progress in applying large-scale models to the video retrieval domain [30, 51].

Masked video modeling (MVM) [23, 77] involves masking random tubes [2, 79] and reconstructing the missing regions for pixel-level reconstruction (Fig. 1(a)). To facilitate the comprehension of local semantics by the Vision Transformer (ViT) [18], a substantial proportion of patches in the tube are masked to reduce temporal redundancy. As depicted in Fig. 1(b), several methods [37, 55, 73, 93] employ MVM in video-text learning by adopting similar random masking strategies and using textual output as the reconstructed target to facilitate high-level perception extraction. However, determining which regions to mask for masked video prediction and learning text-related local content in the video remains challenging. We argue that random masking is inefficient in capturing text-related content. Since the masking is random, the unmasked parts [40] can still reveal the identity of visual concepts and aligned textual content. Furthermore, using the same reconstruction strategy to handle different masked regions also hinders model learning.

To address these limitations, we propose mask for semantics completion, called **MASCOT**, which utilizes a dual-completer to enhance local text-aligned correlations for masked semantics prediction. By leveraging self-attention in ViT, we can discern intrinsic relationships and generate masks for video tubes based on the attention map. The tokens that receive the most attention emphasize both video information and regions that are semantically similar to the text. Consequently, we introduce attention-based video masking to create different masks, with high-informed masks concealing more discriminative cues and low-informed masks disregarding areas containing irrelevant textual content.

*Equal contributions.

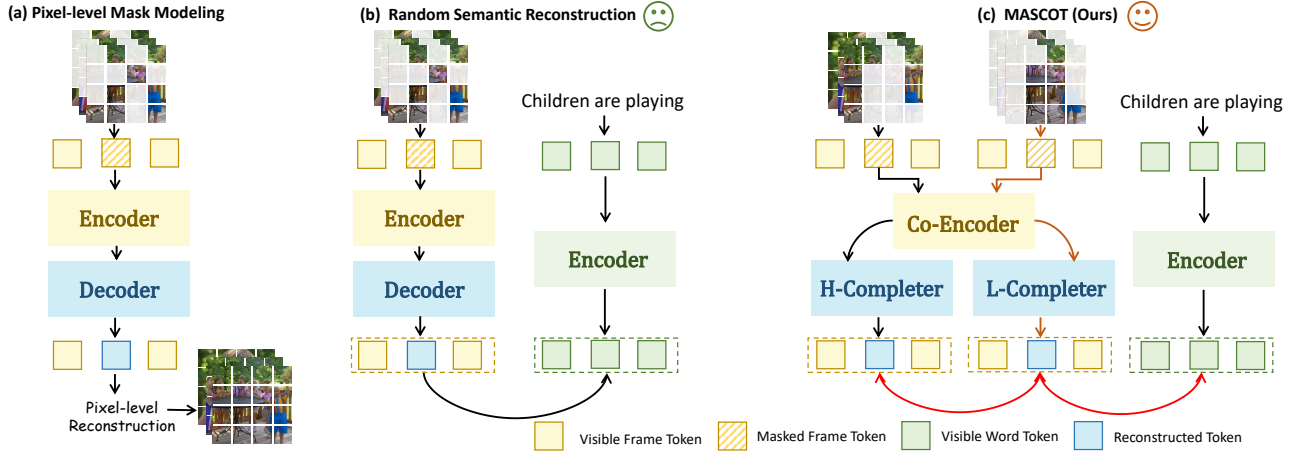


Figure 1. (a) Mask for pixel-level reconstruction. (b) Employing random mask tubes for feature reconstruction. (c) Our MASCOT applies the low-informed and high-informed mask for prediction, prompting to understand the textual-aligned regions.

To fully capture local content related to the text in videos, we employ video and text encoders to construct unmasked video and textual representations for building masked video prediction targets. As shown in Fig. 1(c), we use the spatial encoder as a co-encoder and feed the masked videos to model masked visual representations. Then, the proposed dual-completer is employed to remove noise, by reasoning corrupted details from the correlation of neighboring visible patches. Specifically, unidirectional interaction is incorporated into the attention mechanism of the co-encoder and H-completer. The masked tokens can interact with unmasked tokens, leveraging all visible tokens to recover text-related semantics, while the attention interaction of unmasked tokens is unidirectionally neglected for de-noising. To disregard attention irrelevant to the text with low-informed masks, we introduce a shift of the reconstructed prediction with the L-completer from unaligned backgrounds to discriminative parts. Furthermore, we unify both two types of completions. A novel co-learning strategy is presented to provide more text-related attention distribution and integrate video cues.

In summary, our work contributes in four main ways: **(1)** We propose a new perspective of assembling video-language learning and MVM to align with text-related patches in the video. **(2)** We introduce a novel video masking strategy that integrates textual content to generate high-informed and low-informed masks. **(3)** We propose a novel co-learning strategy to incorporate masking and reconstructed strategies with informed semantics completion and background attention shift. **(4)** We conduct extensive experiments and show that our MASCOT achieves new records on MSR-VTT (54.8%), LSMDC (28.0%), ActivityNet (53.9%), and DiDeMo (52.3%).

2. Related Works

Video-text Retrieval. Existing methods for video-text retrieval [19, 20, 49] utilize multiple representations from different modalities as input and employ fusion networks [84, 97]. The video representation is integrated to align with the text content extracted by text encoders, such as BERT [15]. Recently, researchers have focused on designing intensive cross-modal alignment mechanisms by incorporating pre-trained CLIP [69] for video-language alignment. Since CLIP contains generalized content, CLIP4Clip [53], CLIP2video [22], and STAN [46] transfer the cross-modal correlations to the video level, employing various temporal modeling blocks. DRL [80], X-CLIP [54], and X-pool [31] propose token-level interaction to adaptively exploit pair-wise correlations. Moreover, Ts2Net [50], CenterCLIP [99], and CLIP-ViP [94] incorporate spatial-temporal patch contexts into the vision encoder. In contrast to these methods, we propose masking text-related video tubes and reconstructing them to encourage the model to capture fine-grained semantic relations at both spatial and temporal levels.

Masked Vision Modeling. Masked visual encoders have been proposed to introduce masked visual modeling for self-supervised learning. Masked Image Modeling (MIM) [35] masks a certain proportion of random 2D patches and optimizes the encoder and decoder for pixel-level reconstruction. BEiT [4] converts the image into a discrete sequence of tokens for masked token prediction, rather than directly recovering pixels. MVP [85] introduces multi-modality guided teacher models in MIM, utilizing CLIP [69] features as the reconstruction target. Moreover, masked video modeling [23, 76, 77] has been widely exploited by extending 2D masks into the video domain. VideoMAE [77] proposes a tube mask strategy and achieves

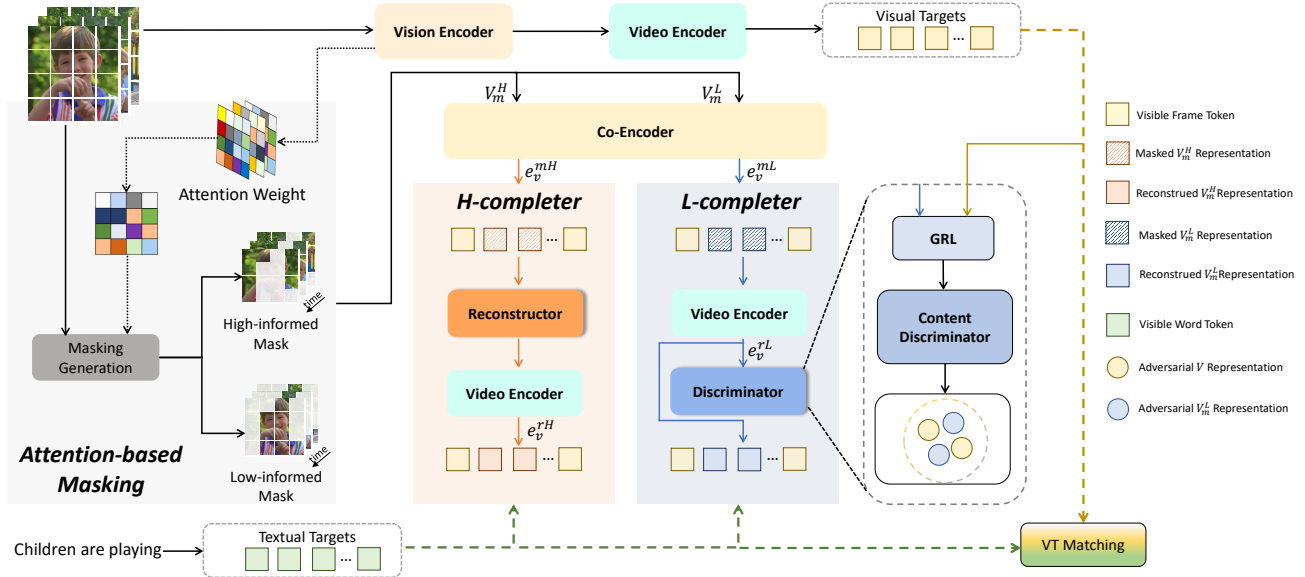


Figure 2. Overview of MASCOT. With the attention-based masking strategy, co-learning of the dual-completer is proposed, including Informed Semantics Reconstruction and Background Attention Shift. GRL represents gradient reversal layer [26].

promising performance with a high mask ratio. MVD [82] suggests a two-stage masked feature modeling framework, employing knowledge distillation for the student model to predict high-level features from teacher models. In contrast, our MASCOT masks video patches for semantic completion and focuses on reconstructing salient regions, without relying on random masking.

Masked Modeling for Cross-modal Alignment. Masked video modeling has been preliminarily explored in video-text alignment for feature-level completion. MILES [30] employs a snapshot video encoder updated by EMA [36] to produce reconstruction targets for handling randomly masked tubes. VidLP [73] introduces a simple framework for masking both video and text tokens, reducing spatial and temporal redundancy to enhance pre-training efficiency. In contrast to these methods, which adopt random masking and apply the same reconstruction strategy for various masked videos, our MASCOT generates high-informed and low-informed masks to intentionally mask text-related patches. Furthermore, we propose a dual-completer to address corrupted videos under different masks and capture more cross-modal content at the patch level.

3. Method

3.1. Overview

As illustrated in Fig. 2, we adopt a two-stream encoder to encode video and text separately. We uniformly sample M frames as video clips and feed unmasked video tokens into the vision transformer, along with temporal transform-

ers [53], to model spatial and temporal information, generating video targets $e_v = \{v_0, v_1, \dots, v_{M-1}\}$. In text encoding, each text is appended with two special tokens, $\langle \text{SOS} \rangle$ and $\langle \text{EOS} \rangle$, and fed into the text encoder to embed textual representations $e_t = \{t_{\text{SOS}}, t_1, \dots, t_{N-2}, t_{\text{EOS}}\}$ as textual targets, with N denoting the text token number. Besides, we employ weighted token interaction (WTI) [80] to calculate the token similarity, fully exploiting the pair-wise token correlations and maximizing the similarity between positive pairs based on all tokens.

3.2. Attention-based Video Masking

Videos exhibit repetitive patterns in both spatial and temporal dimensions, allowing randomly masked areas to be easily restored by their neighboring regions. To enhance local semantic reasoning from unrelated patches, we propose attention-based tube masking, enabling the model to recover masked semantics by relating textual and unmasked visual information. Specifically, we begin by creating a 2D mask for each frame. Each frame is divided into $n = hw/p^2$ non-overlapping patches, where h and w represent the image sizes, and p denotes the patch size. The patches are then projected into d -dimensional tokens, with the CLS token Z^{CLS} prepended to extract the global representation, forming $Z \in \mathbf{R}^{(n+1) \times d}$. Then, multi-head self-attention (MSA) maps in the vision transformer are exploited:

$$\mathcal{A}^l = \frac{1}{H} \sum_{i=1}^H \text{softmax}(Q_i^l K_i^{l\top} / \sqrt{d/H}), \quad (1)$$

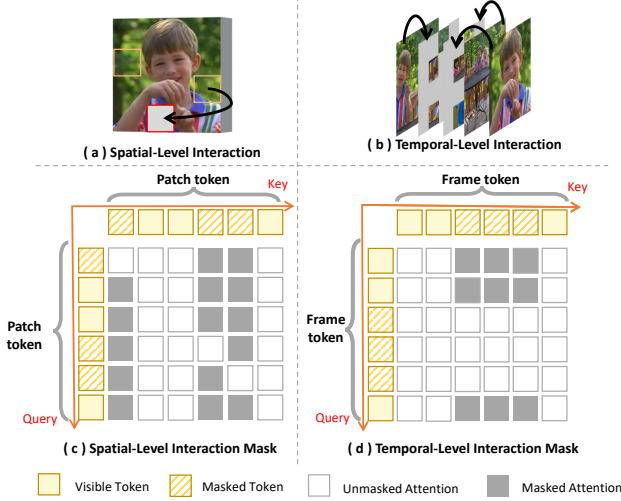


Figure 3. Spatial patch and temporal tube attention interaction. The masked tokens can interact with unmasked tokens, for unidirectional semantics completion, while the attention interaction of unmasked tokens is partially neglected.

where Q and K represent the query and key transformed by tokens Z^l . l denotes the l -th layer of MSA, and H refers to the number of heads. In each layer, the correlation between each patch is modeled to provide the attention matrix averaged over all heads. To emphasize the relations between local regions and the global representation, we use the first row of the matrix (excluding the first element) as the attention weight: $w^l = \{w_{cls-1}, w_{cls-2}, \dots, w_{cls-n}\}$. To extend the attention weight to the 3D tube, we randomly sample two values a_H^s and a_H^e to indicate the start and end of the masked tube. The attention weights are then averaged over the masked tube, with each weight representing the relevance of the region concerning both the global video information and textual content. To obscure more discriminative cues, we generate high-informed masks based on the attention weight's descending order. We choose a number $k = \lfloor r_H \cdot n \rfloor$, which is proportional to the number of patches with a mask ratio of $r_H \in [0, 1]$. We erase the top- k patches by replacing them with random pixels and repeat them in the temporal dimension to obtain V_m^H , where the same spatial patches are masked for each frame in the masked video tube, leading to a more challenging masked video prediction. Similarly, we generate low-informed masks by sorting the weight in ascending order. The regions containing irrelevant textual content are masked with the masked spatial ratio of $r_L \in [0, 1]$ and masked temporal interval a_L^s and a_L^e to generate V_m^L .

3.3. Informed Semantics Reconstruction

Masked semantic completion encourages the model to focus on cross-modal details at the patch level by provid-

ing masked video prediction and reconstructing semantics through correlations between neighboring visible patches. In this section, we utilize the more challenging masked video v_m^H , where the masks conceal the majority of cross-modal content. To eliminate noise from masked salient regions, we propose a co-encoder and H-completer with a novel unidirectional interaction for recovering masked text-related semantics. Specifically, we follow a four-step process: **first**, the co-encoder (spatial encoder) is employed to model spatial information e_v^{mH} and recover semantics at the spatial level. **Second**, a reconstructor is proposed for denoising encoding at the temporal level. **Third**, the reconstructed output is fed into the temporal transformer (Video Encoder) to obtain the reconstructed video representation e_v^{rH} as the prediction. **Finally**, reconstruction is applied to minimize the semantic distance with visual and textual targets.

To fully explore the correlation of local patches and temporal tubes, we propose unidirectional interaction and impose it into every layer of co-encoder and reconstructor. The attention calculation at i -th row and j -th column of l -th layer can be seen as follows:

$$\mathcal{P}_s^l(i, j) / \mathcal{F}_t^l(i, j) = [(A^l \odot \mathcal{U}_{s/t}^l) \otimes V^l](i, j) = \sum_{k=1}^K a_{ik}^l u_{ik}^l v_{kj}^l, \quad (2)$$

where \odot and \otimes denote element-wise and matrix multiplication, $\mathcal{U}_{s/t}^l$ indicates spatial (\mathcal{U}_s^l) and temporal (\mathcal{U}_t^l) interaction mask, \mathcal{P}_s^l is the attention output of co-encoder, and \mathcal{F}_t^l is the attention output of reconstructor. A and V denote the attention weight and value respectively. In spatial encoding, all the attention calculations are the same as the original vision encoding in CLIP [69], except for adding spatial interaction masks. As depicted in Fig. 3(c), the masked tokens adopted as the query, can attend all the unmasked neighboring patch tokens including global cls token, while the unmasked tokens are only allowed to interact with visible information for de-noising. Specifically, we denote the patch tokens in co-encoders as $P = \{p_{cls}^u, p_1^u, p_2^m, p_3^m, \dots, p_n^u\} \in \mathbb{R}^{(n+1) \times d}$, where p^m represents the masked token and p^u represents the unmasked token. The spatial interaction mask is calculated as:

$$\mathcal{U}_s(i, j) = \begin{cases} 0 & p_j \in p^m (i \neq j), \\ 1 & \text{otherwise,} \end{cases} \quad (3)$$

where the value of 0 indicates that attention is neglected, 1 represents the adoption of attention, and i and j represent the index of token p . The representation of masked tokens has limited effects on unmasked regions. By unidirectional interaction, the model is trained to reconstruct masked regions using unmasked cues.

Before feeding the input into the video encoder for temporal modeling, we employ a single-layer self-attention layer as the reconstructor for completion at the temporal level. The reconstructor accepts the output of the co-encoder $e_v^{mH} = \{v_0^u, v_1^m, v_2^m, \dots, v_{M-1}^u\}$, where v^u and v^m denote the unmasked frame tokens and the frame tokens encoded by the masked portions of patches, respectively. We treat each frame token the same as the patch token and impose temporal interaction masks into the reconstruction process.

As depicted in Fig. 3(d), temporal interaction enables mutual attention among masked tokens, since the representation of masked frame tokens is partially recovered. This mask is formulated as:

$$\mathcal{U}_t(i, j) = \begin{cases} 0 & v_i \in v^u, v_j \in v^m, \\ 1 & \text{otherwise.} \end{cases} \quad (4)$$

This completion enables that reconstructing video representation from high-informed masks, providing a more challenging prediction for capturing the fine-grained semantics at the patch level.

3.4. Background Attention Shift

To emphasize the modeling of salient regions, we introduce Background Attention Shift in conjunction with generated low-informed masks. The L-completer, which consists of the video encoder and content discriminator, is utilized to facilitate the shift of the reconstructed target from unaligned backgrounds to more discriminative parts. The video representation $e_v^{rL} = \{v_0^L, v_1^L, \dots, v_{M-1}^L\}$ is generated by feeding V_m^L into the co-encoder and the temporal transformer for low-informed video prediction. Unlike reconstructing representation from V_m^H , we only employ spatial reconstruction within the co-encoder. We conjecture that there are minor distribution discrepancies between unmasked e_v and masked e_v^{rL} based on the following observations: 1. The masked regions, selected based on low attention weight, exhibit limited correlation with global *cls* tokens. The videos, which lose irrelevant information, can still reveal the intrinsic identity; 2. The video obscured by low-informed masks can be easily recovered by applying unidirectional interaction from discriminative neighbors to text-irrelevant patches.

Therefore, we adopt adversarial learning to make low-informed video representation e_v^{rL} indistinguishable from visual targets. The co-encoder and video encoder are optimized by maximizing the adversarial loss functions, while the content discriminator is trained in the opposite direction. Thus, this process can be formulated as:

$$\min_D \max_G \mathcal{L}_{adv}(G, D) = \mathbf{E}_{(x,y)} \sum_{i=1}^{\mathcal{D}} \mathbf{1}[i = y] \log(D(G(x))), \quad (5)$$

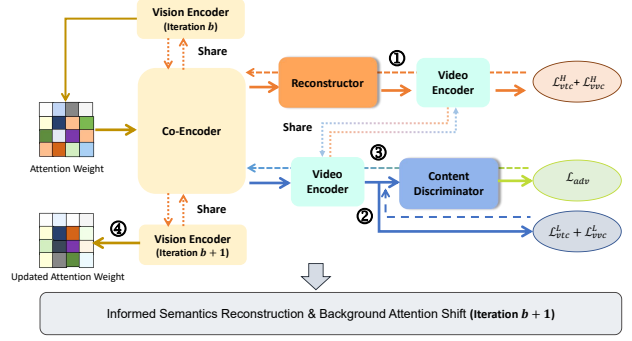


Figure 4. The four-step training scheme ‘‘Co-Learning’’. The solid line and dashed line represents forward and back propagation. The dotted line indicates parameter sharing.

where y denotes the set of labels indicating masked and unmasked output, while \mathcal{D} represents the number of domains. G and D correspond to the feature generation process and content discriminator. To simultaneously optimize G and D , the gradient reversal layer (GRL) [26] is employed, reversing the gradient by multiplying it with a negative scalar during backward propagation. By employing adversarial learning, indistinguishable distributions between e_v^{rL} and e_v are obtained, encouraging the model to disregard the semantics of irrelevant backgrounds and shift the attention distribution, enhancing the correlation between modality-aligned regions.

3.5. Dual-masking Co-learning

To unify different completions and generate masks more relevant to cross-modal content for prediction, we design a collaborative learning strategy called co-learning, as illustrated in Fig. 4. Co-learning consists of four learning branches for each iteration. **First**, the H-completer is updated by processing the masked video v_m^H for informed semantics reconstruction. **Second**, the video encoder within the L-completer is updated by processing the masked video v_m^L for contrastive learning. **Third**, the gradient of \mathcal{L}_{adv} is used to update the content discriminator and reversed to enhance attention shift for the video and spatial encoder. **Finally**, the spatial encoder, which shares parameters with the co-encoder, is also updated to provide a more fine-grained distribution for attention-based masking in the subsequent iteration. Overall, co-learning allows the branches to mutually promote each other. By recovering high-informed and low-informed masked regions, the model is trained to concentrate on modeling text-aligned regions and discard attention to irrelevant backgrounds. Consequently, the training objective of contrastive loss based on WTI [80] can be

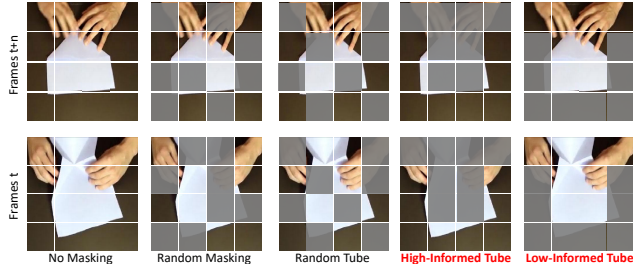


Figure 5. An illustration of different masking strategies.

formulated as:

$$\mathcal{L}_{x_1 2 x_2} = -\frac{1}{B} \sum_i^B \log \frac{\exp(\text{WTI}(\mathbf{e}_{x_1, i}, \mathbf{e}_{x_2, i}) / \tau)}{\sum_j^B \exp(\text{WTI}(\mathbf{e}_{x_1, i}, \mathbf{e}_{x_2, j}) / \tau)}, \quad (6)$$

$$\mathcal{L}_{x_2 2 x_1} = -\frac{1}{B} \sum_i^B \log \frac{\exp(\text{WTI}(\mathbf{e}_{x_2, i}, \mathbf{e}_{x_1, i}) / \tau)}{\sum_j^B \exp(\text{WTI}(\mathbf{e}_{x_2, i}, \mathbf{e}_{x_1, j}) / \tau)}, \quad (7)$$

$$\mathcal{L}_{x_1 x_2 c} = \frac{1}{2} (\mathcal{L}_{x_1 2 x_2} + \mathcal{L}_{x_2 2 x_1}), \quad (8)$$

where \mathbf{e}_{x_1} and \mathbf{e}_{x_2} are the output tokens of different modalities and $\mathcal{L}_{x_1 2 x_2}$ is optimized to minimize the distance between two token sequences. The batch size is represented by B , and τ denotes the temperature. In our method, we adopt both visual and textual targets as objectives and present training reconstruction targets as:

$$\mathcal{L}_{total} = \mathcal{L}_{vtc} + \alpha(\mathcal{L}_{vtc}^H + \mathcal{L}_{vvc}^H) + \beta(\mathcal{L}_{vtc}^L + \mathcal{L}_{vvc}^L) + \gamma \mathcal{L}_{adv}, \quad (9)$$

where \mathcal{L}_{vtc}^L and \mathcal{L}_{vtc}^H represent loss within pairs between masked video and textual target. \mathcal{L}_{vvc}^L and \mathcal{L}_{vvc}^H is optimized by pulling masked video and visible video targets together in embedding space.

4. Experiment

4.1. Experimental Setting

Datasets. *MSR-VTT* [90] comprises 10,000 videos, each of which contains 20 captions. We adopt two training splits, referred to as 7k [58] and 9k [25], which consist of 7,000 and 9,000 videos, respectively. For evaluation, we use the 1K-A test set [97], which includes 1,000 videos. *LSMDC* [71] is made up of 118,081 videos sourced from 202 movies, with 1,000 videos selected for evaluation. *DiDeMo* [1] includes over 10,000 videos, of which 8,395 videos are used for training and 1,004 videos for testing. Following [44, 47, 53], we concatenate all descriptions of a video into a single caption and treat this dataset as a video-paragraph retrieval task. *ActivityNet Captions* [43] comprises 20k videos with 100k dense descriptions. Following the video-paragraph retrieval setting [49, 98], we train our models on 10k videos and test on 4.9k videos.

Table 1. Ablation studies on the masking strategy. "Rand" is shortened for "random mask". "Tube" denotes that the masking the same patches along the temporal dimension. Text-video retrieval on MSR-VTT-9k [25] are evaluated.

Masking	Ratio	Text \Rightarrow Video			Video \Rightarrow Text			Rsum
		R@1	R@5	R@10	R@1	R@5	R@10	
-	-	46.6	73.4	83.5	45.4	73.4	81.9	404.2
Rand	50%	45.8	74.9	83.3	45.0	72.9	83.8	405.7
Rand	70%	46.2	75.5	83.6	44.6	73.4	83.7	407.0
Rand + Tube	50%	47.6	73.3	83.3	45.3	75.2	83.3	408.0
Rand + Tube	70%	47.1	75.4	84.3	44.5	74.7	83.2	409.2
Low-informed	50%	47.9	75.5	83.7	46.0	74.3	84.4	411.8
Low-informed	70%	47.3	74.7	83.5	45.2	73.6	83.9	408.2
High-informed	50%	47.8	75.5	84.1	46.2	74.5	83.3	411.4
High-informed	70%	48.0	75.7	84.0	46.2	74.7	84.5	413.1

Evaluation Metric. Following standard video-text retrieval metrics [57, 60, 98], we report Recall at rank K (R@K), median rank (Mdr) and mean rank (Mnr) as metrics, where K=1, 5, 10 are calculated. The higher R@K, lower median rank and mean rank indicate better performance. Besides, we also sum up all the R@K results as Rsum [50] to indicate the overall performance.

Implementation Details. We employ the vision and text encoder, initialized by CLIP, to encode frame and word tokens. The backbone of MASCOT is ViT-B/32, with a patch size p of 32. Then, we adopt a 4-layer temporal transformer with 8 heads and 512 channels, included in both the H-completer and L-completer. Two linear projections encode the different modalities into a 512-dimension space to match their representations. For MSR-VTT [90] and LSMDC [71], the video and caption lengths are set to 12 and 32, respectively. Following existing methods [49, 98], we set both video and caption lengths to 64 for DiDeMo [1] and ActivityNet [43]. Our MASCOT is trained using the Adam optimizer with a cosine schedule decay and a batch size of 128. For MSR-VTT [90] and LSMDC [71], we train for 5 epochs, while for DiDeMo [1] and ActivityNet [43], we train for 10 epochs. Besides, the learning rate is set to 1e-7 for the frame encoder and text encoder and 1e-4 for the proposed modules. We utilize the final MSA layer of ViT as attention weight and set the mask ratios r_H and r_L to 0.7 and 0.5, respectively, while the temporal intervals a_L^s , a_L^e , a_H^s , and a_H^e are randomly set within the maximum video length. Additionally, we set α , β , and γ to 0.5, 0.5, and 0.2, respectively, to control the weight of loss functions.

4.2. Ablation Experiments

Video masking strategy. The diverse video masking strategies are investigated, with visualizations displayed in Fig. 5. Random masking independently conceals random patches for each frame, while tube-based masking obscures the same blocks along the temporal dimension. In Tab. 1, by employing informed semantics completion for

Table 2. Effects of different components, where the text-video retrieval results are evaluated on MSR-VTT-9k [25]. "V" and "T" represents the co-encoder and video encoder. "D" denotes the discriminator. "R" denotes the reconstructor. "V_u" and "R_u" indicates that co-encoder and reconstructor with unidirectional interaction. "H + L" represents co-learning.

Method	Text ⇒ Video			Video ⇒ Text			Rsum
	R@1	R@5	R@10	R@1	R@5	R@10	
<i>H-completer</i>							
$T + V$	47.1	75.0	83.2	45.5	73.9	83.2	407.9
$T + V + R$	47.5	75.5	83.6	46.2	74.5	83.8	411.1
$T + V + R_u$	47.8	75.7	83.5	46.1	74.6	84.0	411.7
$T + V_u + R$	47.9	75.5	83.8	46.0	74.7	84.3	412.2
$T + V_u + R_u (H)$	48.0	75.7	84.0	46.2	74.7	84.5	413.1
<i>L-completer</i>							
$T + V$	47.6	75.0	83.4	45.7	73.4	83.4	408.5
$T + V + R_u$	47.2	74.4	83.6	45.0	73.1	83.5	406.8
$T + V_u$	47.5	75.1	83.5	45.6	73.7	83.9	409.3
$T + V + D$	47.4	75.3	83.7	45.8	74.2	84.0	410.4
$T + V_u + D (L)$	47.9	75.5	83.7	46.0	74.3	84.4	411.8
<i>Co-learning</i>							
$H + L$	48.3	75.8	84.4	46.6	74.4	85.0	414.5

reconstruction, random masks yield the worst results. Using tube-based masking for the model to reason masked semantics solely from neighboring patches proves more effective. Additionally, high-informed masks deliberately conceal regions containing salient cross-modal content, pushing the model to temporally and spatially integrate visible patches for fine-grained reconstruction at the patch level. Conversely, low-informed masking for background attention shift demonstrates less satisfactory performance, indicating that reasoning the masked text-related patches is essential. We also investigate the impact of the mask ratio and observe that both high-informed and low-informed masks perform well at ratios of 70% and 50%, respectively. It is found that creating a more difficult high-informed reconstruction task improves model learning. However, masking too many text-irrelevant regions for attention shift may result in the neglect of crucial semantic information.

Effects of H-completer. We explore various structures of H-completer for informed semantic completion, including the reconstructor, and spatial and temporal interaction mask. As depicted in the upper part of Tab. 2, incorporating a reconstructor between the co-encoder and video encoder yields a substantial improvement. This result indicates that temporal relations act as crucial cues for predicting masked video patches. Consequently, the model enhances its reasoning ability regarding local spatial correlation at the temporal level, while the video encoder can be focused on temporal modeling. Furthermore, we introduce unidirectional interaction and apply it to both the co-encoder and reconstructor. The masked tokens are adopted as query to interact with unmasked tokens in spatial interaction and all the features in temporal interaction for completion, leverag-

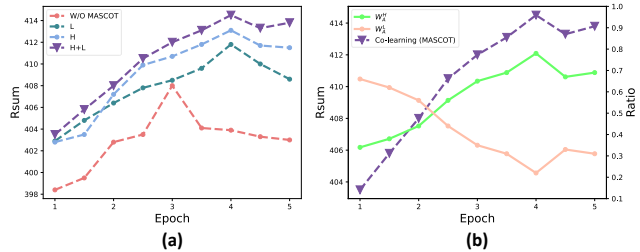


Figure 6. (a) Analysis of Rsum with co-learning. "W/O MASCOT" represents without reconstruction. (b) Attention weight versus performance in MSR-VTT-9k [90]. W_A^H and W_A^L represent the top and bottom 30% of attention weights.

ing all visible video cues. Meanwhile, the attention interactions of visible correlation are only allowed between the unmasked tokens for unidirectional de-noising. Compared to full attention ($T + V + R$), the inclusion of unidirectional interaction ($T + V_u + R_u$) results in further performance enhancement. Similar improvement is observed in the middle of Tab. 2, where spatial interaction ($T + V_u$) is imposed for background attention shift.

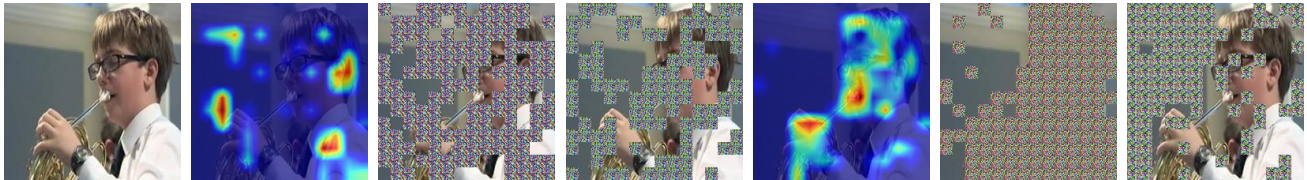
Effects of L-completer. It is worth noting that incorporating a reconstructor in the L-completer yields inferior results compared to solely adopting a "spatial-video" structure. This can be attributed to the fact that focusing on reconstructing text-irrelevant regions does not enhance the semantic correlation at the patch level, leading to decreased performance. As videos masked by low-informed masks still reveal sufficient intrinsic identity for cross-modal alignment, we employ the content discriminator D to minimize the representation difference. The model is encouraged to learn indistinguishable feature distributions between unmasked and masked representations without reconstruction. Consequently, the masked video representation, obscured by regions with low attention weight, demonstrates a similar performance to unmasked videos by mitigating the effects of patch masking. This suggests that the model identifies and disregards more text-irrelevant information, achieving attention shifting towards regions with more cross-modal content.

Effects of Co-learning. To demonstrate the effectiveness of incorporating both H-completer and L-completer, we present the results of co-learning ($H + L$) at the bottom of Tab. 2, which achieves significant improvement. Co-learning enables the two completions to complement each other by discarding semantics of irrelevant backgrounds and focusing more on completing the masked semantics of cross-modal content. In Fig. 6(a), we illustrate the performance curves across different epochs. The performance without MASCOT initially increases when transferring image representations into videos but rapidly decreases afterward, indicating that the model suffers from overfitting due to limited training data. However, by gradually adding the

Table 3. Retrieval performance comparison trained on MSR-VTT-9k [90] and evaluated on 1k-A test. * means adopting DSL [12] as extra trick during inference.

Method	R@1	R@5	R@10	MdR	MnR	R@1	R@5	R@10	MdR	MnR
CE [49]	20.9	48.8	62.4	6.0	28.2	20.6	50.3	64.0	5.3	25.1
MMT [25]	26.6	57.1	69.6	4.0	24.0	27.0	57.5	69.7	3.7	21.3
SUPPORT-SET [66]	27.4	56.3	67.7	3.0	-	26.6	55.1	67.5	3.0	-
T2VLAD [84]	29.5	59.0	70.1	4.0	-	31.8	60.0	71.1	3.0	-
FROZEN [3]	31.0	59.5	70.5	3.0	-	-	-	-	-	-
HIT [47]	30.7	60.9	73.2	2.6	-	32.1	62.7	74.1	3.0	-
MDMMT [19]	38.9	69.0	79.7	2.0	16.5	-	-	-	-	-
<i>CLIP-ViT-B/32</i>										
CLIPforward [68]	31.2	53.7	64.2	4.0	-	27.2	51.7	62.6	5.0	-
CLIP4Clip [53]	44.5	71.4	81.6	2.0	15.3	42.7	70.9	80.6	2.0	11.6
CLIP2Video [22]	45.6	72.6	81.7	2.0	14.6	43.5	72.3	82.1	2.0	10.2
QB-Norm [7]	47.2	73.0	83.0	2.0	-	-	-	-	-	-
STAN [46]	46.9	72.8	82.8	2.0	-	-	-	-	-	-
STAN* [46]	49.0	74.8	83.5	2.0	-	-	-	-	-	-
CAMOE* [12]	47.3	74.2	84.5	2.0	11.9	49.1	74.3	84.3	2.0	9.9
X-pool [31]	46.9	72.8	82.2	2.0	14.3	-	-	-	-	-
X-CLIP [54]	46.1	73.0	83.1	2.0	13.2	46.8	73.3	84.0	2.0	9.1
TS2Net [50]	47.0	74.5	83.8	2.0	13.0	45.3	74.1	83.7	2.0	9.2
DRL [80]	47.4	74.6	83.8	2.0	-	45.3	73.9	83.3	2.0	8.7
MASCOT (Ours)	48.3	75.8	84.4	2.0	12.6	46.6	74.4	85.0	2.0	9.1
MASCOT* (Ours)	52.5	78.3	85.9	1.0	10.5	52.8	78.2	86.3	1.0	8.6
<i>CLIP-ViT-B/16</i>										
CLIP2TV [29]	48.3	74.6	82.8	2.0	14.9	46.5	75.4	84.9	2.0	10.2
CenterCLIP [99]	48.4	73.8	82.0	2.0	13.8	47.7	75.0	83.3	2.0	10.2
TS2Net [50]	49.4	75.6	85.3	2.0	13.5	46.6	75.9	84.9	2.0	8.9
X-CLIP [54]	49.3	75.8	84.8	2.0	13.2	48.9	76.8	84.5	2.0	8.1
DRL [80]	50.2	76.5	84.7	1.0	-	48.9	76.3	85.4	2.0	-
STAN [46]	50.0	75.2	84.1	1.5	-	-	-	-	-	-
STAN* [46]	54.1	79.5	87.8	1.0	-	-	-	-	-	-
MASCOT (Ours)	50.5	77.6	85.2	1.0	11.2	49.5	77.3	86.4	2.0	8.0
MASCOT* (Ours)	54.8	80.3	87.7	1.0	9.6	54.9	79.4	87.6	1.0	7.3

Caption: a young boy plays an instrument



Caption: man folding a green paper into a paper airplane

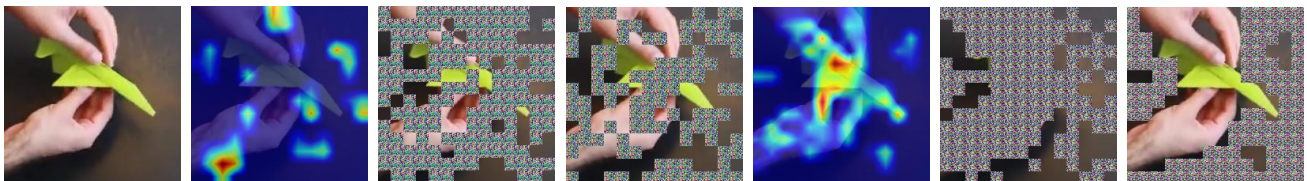


Figure 7. Att , V_m^H , and V_m^L represent the attention map, video masked by high-informed and low-informed mask, where the results in columns 2-4 and columns 5-7 are initialized by CLIP [69] and obtained after training with MASCOT, respectively.

H-completer and L-completer, Rsum improves and eventually stabilizes, which signifies the robustness of mitigating overfitting by introducing challenging masked video predic-

tion. Furthermore, we visualize the change of average attention weight for attention-based masking in Fig. 6(b). The top 30% (W_A^H) and bottom 30% (W_A^L) attention weights

Table 4. Text-to-video results on MSR-VTT-7k [58]. * means adopting DSL [12] as extra trick during inference.

Method	R@1	R@5	R@10	MdR	MnR
ClipBERT [44]	22.0	46.8	59.9	6.0	-
CLIP4Clip [53]	42.1	71.9	81.4	2.0	16.2
X-Pool [31]	43.9	72.5	82.3	2.0	14.6
MASCOT (Ours)	45.8	73.0	83.1	2.0	13.9
MASCOT* (Ours)	47.2	75.8	85.3	2.0	12.4

Table 5. Text-to-video results on LSMDC [71] testing set. * means adopting DSL [12] as extra trick during inference.

Method	R@1	R@5	R@10	MdR	MnR
MDMMT [19]	18.8	38.5	47.9	12.3	58.0
CLIP4Clip [53]	22.6	41.0	49.1	11.0	61.0
STAN [46]	23.7	42.7	51.8	9.0	-
DRL [80]	24.9	45.7	55.3	7.0	-
STAN* [46]	26.2	46.0	53.9	9.0	-
CAMOE* [12]	25.9	46.1	53.7	-	54.4
MASCOT (Ours)	25.9	47.5	58.0	7.0	44.7
MASCOT* (Ours)	28.0	48.1	58.8	6.0	43.3

Table 6. Text-to-video results on DiDeMo [1] testing set. * means adopting DSL [12] as extra trick during inference.

Method	R@1	R@5	R@10	MdR	MnR
TeachText [14]	21.1	47.3	61.1	6.3	-
CLIP4Clip [53]	43.4	70.2	80.6	2.0	17.5
TS2-Net [50]	41.8	71.6	82.0	2.0	14.8
STAN [46]	46.2	70.4	80.0	2.0	-
STAN* [46]	51.3	75.1	83.4	1.0	-
MASCOT (Ours)	48.1	75.7	85.1	2.0	11.8
MASCOT* (Ours)	52.0	78.3	85.3	1.0	10.0

Table 7. Text-to-video results on ActivityNet [43] testing set. * means adopting DSL [12] as extra trick during inference.

Method	R@1	R@5	R@10	MdR	MnR
ClipBERT [44]	21.3	49.0	63.5	6.0	-
MMT [25]	28.7	61.4	-	3.3	16.0
CLIP4Clip [53]	40.5	72.4	-	2.0	7.5
TS2-Net [50]	41.0	73.6	84.5	2.0	8.4
MASCOT (Ours)	45.4	76.1	87.2	2.0	5.8
MASCOT* (Ours)	53.9	81.0	89.9	1.0	4.9

are depicted, which are used to generate high-informed and low-informed masks. As performance increases, the top and bottom attention weights increase and decrease, respectively. This indicates that the model’s learning focus has indeed shifted from irrelevant patches to regions containing more cross-modal content, leading to better performance.

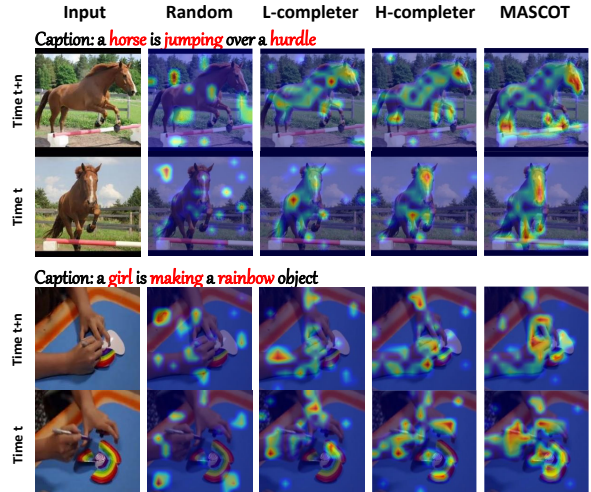


Figure 8. The visualizations of attention weight in the co-encoder. "Random" means adopting random masks for reconstruction. "L-completer" and "H-completer" are based on low and high-informed masks, respectively, while MASCOT unifies both two masks and corresponding reconstruction strategies to capture text-aligned visual semantics.

4.3. Comparisons with State-of-the-art Models

To fairly evaluate the performance of our proposed MASCOT, we compare it with other state-of-the-art methods on four datasets: MSR-VTT [90], LSMDC [71], DiDeMo [1], and ActivityNet [43]. The text-to-video results are presented in Tab. 3, 4, 5, 6, and 7. As observed, our method outperforms the previous methods without any extra tricks by a significant margin, improving R@1 by at least **3.0%** across all four benchmarks. Specifically, we achieve **+3.8%** and **+3.3%** higher R@1 than CLIP4Clip [53] with ViT-B/32 on MSR-VTT-9k [90] and LSMDC [71]. Compared to the leading method TS2-Net [50], significant improvements can be observed on DiDeMo [1] (**+6.3%** at R@1) and ActivityNet [43] (**+4.4%** at R@1), where longer video tubes are masked to recover masked prediction and identify text-related semantics. Additionally, the results of MSR-VTT-9k achieved by CLIP-B/16 are reported in Tab. 3, which still outperforms the previous best method. Furthermore, we include results with inverted softmax (DSL [12]), which significantly improves the performance. This indicates that our model learns the generalized video-language alignment at the fine-grained level. The prominent results demonstrate that MASCOT works well on cross-modal pairs.

4.4. Qualitative Results

We present a visualization of the self-attention map obtained from the final layer of the co-encoder, based on ViT-B/16 architecture in Fig. 7. This map is used to

generate both high-informed and low-informed masks. To demonstrate the effectiveness of MASCOT’s masking and reconstruction strategies, we show the changes in the attention map before and after training. Our results show that MASCOT is successful in shifting attention from irrelevant patches to relevant video cues, resulting in the capture of more cross-modal correspondences. Besides, we also provide illustrations of change in the masked frames, where the pixel-level masks are depicted to intentionally obscure semantic-based regions. This indicates that attention-based masking gradually captures more fine cross-modal content for challenging reconstruction with training.

We also present Fig. 8, which visualizes the attention distribution trained using different strategies. Our proposed MASCOT model pays more attention to local regions with text-related content compared to the model with random masks. Specifically, in the first two rows, MASCOT focuses on the hurdle and the shape of a horse, including the movement of horse hooves, while the model with random masks identifies regions of limited content, such as the body and some background, which are not relevant to the caption. By utilizing attention-based masking and incorporating the H-completer and L-completer, MASCOT captures cross-modal content at the local level while neglecting attention to irrelevant regions.

5. Conclusion

We propose **MA**sk for **S**emantics **CO**mple**T**ion, a novel method for video-language learning and masked video modeling. Our method employs attention-based masking to intentionally obscure videos by utilizing high-informed masks for informed semantics reconstruction and low-informed masks for background attention shift. Furthermore, our co-learning strategy incorporates two completions and enhances the fine-grained understanding of video context based on cross-modal content. The proposed method delivers significant improvements across four video-text benchmarks.

References

[1] Lisa Anne Hendricks, Oliver Wang, Eli Shechtman, Josef Sivic, Trevor Darrell, and Bryan Russell. Localizing moments in video with natural language. In *Proceedings of the IEEE international conference on computer vision*, pages 5803–5812, 2017. 1, 6, 9

[2] Anurag Arnab, Mostafa Dehghani, Georg Heigold, Chen Sun, Mario Lučić, and Cordelia Schmid. Vivit: A video vision transformer. In *Proceedings of the IEEE/CVF international conference on computer vision*, pages 6836–6846, 2021. 1

[3] Max Bain, Arsha Nagrani, Gül Varol, and Andrew Zisserman. Frozen in time: A joint video and image encoder for end-to-end retrieval. In *IEEE/CVF International Confer-*

ence on Computer Vision (ICCV), pages 1708–1718, 2021. 8

[4] Hangbo Bao, Li Dong, Songhao Piao, and Furu Wei. Beit: Bert pre-training of image transformers. *arXiv preprint arXiv:2106.08254*, 2021. 2

[5] Anil Bhattacharyya. On a measure of divergence between two multinomial populations. *Sankhyā: the indian journal of statistics*, pages 401–406, 1946.

[6] Simion-Vlad Bogolin, Ioana Croitoru, Hailin Jin, Yang Liu, and Samuel Albanie. Cross modal retrieval with querybank normalisation. In *Proceedings of the IEEE/CVF Conference on Computer Vision and Pattern Recognition (CVPR)*, pages 5194–5205, June 2022.

[7] Simion-Vlad Bogolin, Ioana Croitoru, Hailin Jin, Yang Liu, and Samuel Albanie. Cross modal retrieval with querybank normalisation. In *Proceedings of the IEEE/CVF Conference on Computer Vision and Pattern Recognition*, pages 5194–5205, 2022. 8

[8] Fabian Caba Heilbron, Victor Escorcia, Bernard Ghanem, and Juan Carlos Niebles. Activitynet: A large-scale video benchmark for human activity understanding. In *Proceedings of the IEEE conference on computer vision and pattern recognition*, pages 961–970, 2015. 1

[9] Jie Chang, Zhonghao Lan, Changmao Cheng, and Yichen Wei. Data uncertainty learning in face recognition. In *Proceedings of the IEEE/CVF Conference on Computer Vision and Pattern Recognition*, pages 5710–5719, 2020.

[10] David Chen and William B Dolan. Collecting highly parallel data for paraphrase evaluation. In *Proceedings of the Annual Meeting of the Association for Computational Linguistics: Human Language Technologies*, pages 190–200, 2011. 1

[11] Shizhe Chen, Yida Zhao, Qin Jin, and Qi Wu. Fine-grained video-text retrieval with hierarchical graph reasoning. In *Proceedings of the IEEE/CVF Conference on Computer Vision and Pattern Recognition*, pages 10638–10647, 2020. 1

[12] Xing Cheng, Hezheng Lin, Xiangyu Wu, Fan Yang, and Dong Shen. Improving video-text retrieval by multi-stream corpus alignment and dual softmax loss. *arXiv preprint arXiv:2109.04290*, 2021. 8, 9

[13] Sanghyuk Chun, Seong Joon Oh, Rafael Sampaio De Rezende, Yannis Kalantidis, and Diane Larlus. Probabilistic embeddings for cross-modal retrieval. In *Proceedings of the IEEE/CVF Conference on Computer Vision and Pattern Recognition*, pages 8415–8424, 2021.

[14] Ioana Croitoru, Simion-Vlad Bogolin, Marius Leordeanu, Hailin Jin, Andrew Zisserman, Samuel Albanie, and Yang Liu. Teachtext: Crossmodal generalized distillation for text-video retrieval. In *Proceedings of the IEEE/CVF International Conference on Computer Vision*, pages 11583–11593, 2021. 9

[15] Jacob Devlin, Ming-Wei Chang, Kenton Lee, and Kristina Toutanova. Bert: Pre-training of deep bidirectional transformers for language understanding. *arXiv preprint arXiv:1810.04805*, 2018. 2

[16] Jeff Donahue, Yangqing Jia, Oriol Vinyals, Judy Hoffman, Ning Zhang, Eric Tzeng, and Trevor Darrell. Decaf: A deep

- convolutional activation feature for generic visual recognition. In *International conference on machine learning*, pages 647–655. PMLR, 2014.
- [17] Jianfeng Dong, Xirong Li, Chaoxi Xu, Xun Yang, Gang Yang, Xun Wang, and Meng Wang. Dual encoding for video retrieval by text. *IEEE Transactions on Pattern Analysis and Machine Intelligence*, 2021.
- [18] Alexey Dosovitskiy, Lucas Beyer, Alexander Kolesnikov, Dirk Weissenborn, Xiaohua Zhai, Thomas Unterthiner, Mostafa Dehghani, Matthias Minderer, Georg Heigold, and Sylvain Gelly. An image is worth 16x16 words: Transformers for image recognition at scale. In *Proceedings of the International Conference on Learning Representations*, pages 1–22, 2020. [1](#)
- [19] Maksim Dzabaraev, Maksim Kalashnikov, Stepan Komkov, and Aleksandr Petiushko. MDMMT: multidomain multimodal transformer for video retrieval. In *IEEE Conference on Computer Vision and Pattern Recognition Workshops*, pages 3354–3363, 2021. [1](#), [2](#), [8](#), [9](#)
- [20] Fartash Faghri, David J Fleet, Jamie Ryan Kiros, and Sanja Fidler. Vse++: Improving visual-semantic embeddings with hard negatives. *arXiv preprint arXiv:1707.05612*, 2017. [1](#), [2](#)
- [21] Alex Falcon, Swathikiran Sudhakaran, Giuseppe Serra, Sergio Escalera, and Oswald Lanz. Relevance-based margin for contrastively-trained video retrieval models. In *Proceedings of the 2022 International Conference on Multimedia Retrieval*, pages 146–157, 2022.
- [22] Han Fang, Pengfei Xiong, Luhui Xu, and Wenhan Luo. Transferring image-clip to video-text retrieval via temporal relations. *IEEE Transactions on Multimedia*, 2022. [1](#), [2](#), [8](#)
- [23] Christoph Feichtenhofer, Yanghao Li, Kaiming He, et al. Masked autoencoders as spatiotemporal learners. *Advances in neural information processing systems*, 35:35946–35958, 2022. [1](#), [2](#)
- [24] Zerun Feng, Zhimin Zeng, Caili Guo, and Zheng Li. Exploiting visual semantic reasoning for video-text retrieval. *arXiv preprint arXiv:2006.08889*, 2020.
- [25] Valentin Gabeur, Chen Sun, Karteek Alahari, and Cordelia Schmid. Multi-modal transformer for video retrieval. In *European Conference on Computer Vision (ECCV)*, volume 5. Springer, 2020. [6](#), [7](#), [8](#), [9](#)
- [26] Yaroslav Ganin and Victor Lempitsky. Unsupervised domain adaptation by backpropagation. In *International conference on machine learning*, pages 1180–1189. PMLR, 2015. [3](#), [5](#)
- [27] Peng Gao, Shijie Geng, Renrui Zhang, Teli Ma, Rongyao Fang, Yongfeng Zhang, Hongsheng Li, and Yu Qiao. Clip-adapter: Better vision-language models with feature adapters. *arXiv preprint arXiv:2110.04544*, 2021. [1](#)
- [28] Peng Gao, Teli Ma, Hongsheng Li, Jifeng Dai, and Yu Qiao. Convmae: Masked convolution meets masked autoencoders. *arXiv preprint arXiv:2205.03892*, 2022.
- [29] Zijian Gao, Jingyu Liu, Sheng Chen, Dedan Chang, Hao Zhang, and Jinwei Yuan. Clip2tv: An empirical study on transformer-based methods for video-text retrieval. *arXiv preprint arXiv:2111.05610*, 2021. [8](#)
- [30] Yuying Ge, Yixiao Ge, Xihui Liu, Jinpeng Wang, Jianping Wu, Ying Shan, Xiaohu Qie, and Ping Luo. Miles: visual bert pre-training with injected language semantics for video-text retrieval. In *Computer Vision—ECCV 2022: 17th European Conference, Tel Aviv, Israel, October 23–27, 2022, Proceedings, Part XXXV*, pages 691–708. Springer, 2022. [1](#), [3](#)
- [31] Satya Krishna Gorti, Noël Vouitsis, Junwei Ma, Keyvan Golestan, Maksims Volkovs, Animesh Garg, and Guangwei Yu. X-pool: Cross-modal language-video attention for text-video retrieval. In *Proceedings of the IEEE/CVF Conference on Computer Vision and Pattern Recognition*, pages 5006–5015, 2022. [1](#), [2](#), [8](#), [9](#)
- [32] Alex Graves and Alex Graves. Long short-term memory. *Supervised sequence labelling with recurrent neural networks*, pages 37–45, 2012.
- [33] M. Gutmann and A. Hyvriinen. Noise-contrastive estimation: A new estimation principle for unnormalized statistical models. In *International Conference on Artificial Intelligence and Statistics*, 2010.
- [34] Raia Hadsell, Sumit Chopra, and Yann LeCun. Dimensionality reduction by learning an invariant mapping. In *2006 IEEE Computer Society Conference on Computer Vision and Pattern Recognition (CVPR'06)*, volume 2, pages 1735–1742. IEEE, 2006.
- [35] Kaiming He, Xinlei Chen, Saining Xie, Yanghao Li, Piotr Dollár, and Ross Girshick. Masked autoencoders are scalable vision learners. In *Proceedings of the IEEE/CVF Conference on Computer Vision and Pattern Recognition*, pages 16000–16009, 2022. [2](#)
- [36] Kaiming He, Haoqi Fan, Yuxin Wu, Saining Xie, and Ross Girshick. Momentum contrast for unsupervised visual representation learning. In *Proceedings of the IEEE/CVF conference on computer vision and pattern recognition*, pages 9729–9738, 2020. [3](#)
- [37] Zejiang Hou, Fei Sun, Yen-Kuang Chen, Yuan Xie, and Sun-Yuan Kung. Milan: Masked image pretraining on language assisted representation. *arXiv preprint arXiv:2208.06049*, 2022. [1](#)
- [38] Weizhe Hua, Zihang Dai, Hanxiao Liu, and Quoc Le. Transformer quality in linear time. In *International Conference on Machine Learning*, pages 9099–9117. PMLR, 2022.
- [39] Chao Jia, Yinfei Yang, Ye Xia, Yi-Ting Chen, Zarana Parekh, Hieu Pham, Quoc Le, Yun-Hsuan Sung, Zhen Li, and Tom Duerig. Scaling up visual and vision-language representation learning with noisy text supervision. In *International Conference on Machine Learning*, pages 4904–4916. PMLR, 2021. [1](#)
- [40] Ioannis Kakogeorgiou, Spyros Gidaris, Bill Psomas, Yannis Avrithis, Andrei Bursuc, Konstantinos Karantzas, and Nikos Komodakis. What to hide from your students: Attention-guided masked image modeling. In *Computer Vision—ECCV 2022: 17th European Conference, Tel Aviv, Israel, October 23–27, 2022, Proceedings, Part XXX*, pages 300–318. Springer, 2022. [1](#)
- [41] Omar Khattab and Matei Zaharia. Colbert: Efficient and effective passage search via contextualized late interaction

- over bert. In *Proceedings of the 43rd International ACM SIGIR conference on research and development in Information Retrieval*, pages 39–48, 2020.
- [42] Ryan Kiros, Ruslan Salakhutdinov, and Richard S Zemel. Unifying visual-semantic embeddings with multimodal neural language models. *arXiv preprint arXiv:1411.2539*, 2014.
- [43] Ranjay Krishna, Kenji Hata, Frederic Ren, Li Fei-Fei, and Juan Carlos Niebles. Dense-captioning events in videos. In *Proceedings of the IEEE/ICCV Conference on computer vision*, pages 706–715, 2017. 6, 9
- [44] Jie Lei, Linjie Li, Luwei Zhou, Zhe Gan, Tamara L Berg, Mohit Bansal, and Jingjing Liu. Less is more: Clipbert for video-and-language learning via sparse sampling. In *Proceedings of the IEEE/CVF Conference on Computer Vision and Pattern Recognition*, pages 7331–7341, 2021. 6, 9
- [45] Linjie Li, Yen-Chun Chen, Yu Cheng, Zhe Gan, Licheng Yu, and Jingjing Liu. Hero: Hierarchical encoder for video+ language omni-representation pre-training. *arXiv preprint arXiv:2005.00200*, 2020.
- [46] Ruyang Liu, Jingjia Huang, Ge Li, Jiashi Feng, Xinglong Wu, and Thomas H Li. Revisiting temporal modeling for clip-based image-to-video knowledge transferring. *arXiv preprint arXiv:2301.11116*, 2023. 1, 2, 8, 9
- [47] Song Liu, Haoqi Fan, Shengsheng Qian, Yiru Chen, Wenkui Ding, and Zhongyuan Wang. Hit: Hierarchical transformer with momentum contrast for video-text retrieval. In *Proceedings of the IEEE/CVF International Conference on Computer Vision*, pages 11915–11925, 2021. 6, 8
- [48] S. Liu, H. Fan, S. Qian, Y. Chen, W. Ding, and Z. Wang. Hit: Hierarchical transformer with momentum contrast for video-text retrieval. 2021.
- [49] Yang Liu, Samuel Albanie, Arsha Nagrani, and Andrew Zisserman. Use what you have: Video retrieval using representations from collaborative experts. *arXiv preprint arXiv:1907.13487*, 2019. 1, 2, 6, 8
- [50] Yuqi Liu, Pengfei Xiong, Luhui Xu, Shengming Cao, and Qin Jin. Ts2-net: Token shift and selection transformer for text-video retrieval. In *European Conference on Computer Vision*, pages 319–335. Springer, 2022. 1, 2, 6, 8, 9
- [51] Huaishao Luo, Lei Ji, Botian Shi, Haoyang Huang, Nan Duan, Tianrui Li, Xilin Chen, and Ming Zhou. Univlm: A unified video and language pre-training model for multimodal understanding and generation. *arXiv preprint arXiv:2002.06353*, 2020. 1
- [52] Huaishao Luo, Lei Ji, Botian Shi, Haoyang Huang, Nan Duan, Tianrui Li, Jason Li, Taroon Bharti, and Ming Zhou. Univl: A unified video and language pre-training model for multimodal understanding and generation. *arXiv preprint arXiv:2002.06353*, 2020.
- [53] Huaishao Luo, Lei Ji, Ming Zhong, Yang Chen, Wen Lei, Nan Duan, and Tianrui Li. Clip4clip: An empirical study of clip for end to end video clip retrieval and captioning. *Neurocomputing*, 508:293–304, 2022. 1, 2, 3, 6, 8, 9
- [54] Yiwei Ma, Guohai Xu, Xiaoshuai Sun, Ming Yan, Ji Zhang, and Rongrong Ji. X-clip: End-to-end multi-grained contrastive learning for video-text retrieval. In *Proceedings of the 30th ACM International Conference on Multimedia*, pages 638–647, 2022. 1, 2, 8
- [55] Yue Ma, Tianyu Yang, Yin Shan, and Xiu Li. Simvtp: Simple video text pre-training with masked autoencoders. *arXiv preprint arXiv:2212.03490*, 2022. 1
- [56] Antoine Miech, Jean-Baptiste Alayrac, Lucas Smaira, Ivan Laptev, Josef Sivic, and Andrew Zisserman. End-to-end learning of visual representations from uncurated instructional videos. In *Proceedings of the IEEE/CVF Conference on Computer Vision and Pattern Recognition*, pages 9879–9889, 2020.
- [57] Antoine Miech, Ivan Laptev, and Josef Sivic. Learning a text-video embedding from incomplete and heterogeneous data. *arXiv preprint arXiv:1804.02516*, 2018. 6
- [58] Antoine Miech, Dimitri Zhukov, Jean-Baptiste Alayrac, Makarand Tapaswi, Ivan Laptev, and Josef Sivic. Howto100m: Learning a text-video embedding by watching hundred million narrated video clips. In *Proceedings of the IEEE/CVF International Conference on Computer Vision*, pages 2630–2640, 2019. 6, 9
- [59] Shaobo Min, Weijie Kong, Rong-Cheng Tu, Dihong Gong, Chengfei Cai, Wenzhe Zhao, Chenyang Liu, Sixiao Zheng, Hongfa Wang, Zhifeng Li, et al. Hunyuan_tvr for text-video retrieval. *arXiv preprint arXiv:2204.03382*, 2022.
- [60] Niluthpol Chowdhury Mithun, Juncheng Li, Florian Metze, and Amit K Roy-Chowdhury. Learning joint embedding with multimodal cues for cross-modal video-text retrieval. In *Proceedings of the 2018 ACM on International Conference on Multimedia Retrieval*, pages 19–27, 2018. 6
- [61] Seong Joon Oh, Kevin Murphy, Jiyan Pan, Joseph Roth, Florian Schroff, and Andrew Gallagher. Modeling uncertainty with hedged instance embedding. *arXiv preprint arXiv:1810.00319*, 2018.
- [62] Seong Joon Oh, Kevin Murphy, Jiyan Pan, Joseph Roth, Florian Schroff, and Andrew Gallagher. Modeling uncertainty with hedged instance embedding. *arXiv preprint arXiv:1810.00319*, 2018.
- [63] Aaron van den Oord, Yazhe Li, and Oriol Vinyals. Representation learning with contrastive predictive coding. *arXiv preprint arXiv:1807.03748*, 2018.
- [64] Jungin Park, Jiyoung Lee, Ig-Jae Kim, and Kwanghoon Sohn. Probabilistic representations for video contrastive learning. In *Proceedings of the IEEE/CVF Conference on Computer Vision and Pattern Recognition*, pages 14711–14721, 2022.
- [65] Jungin Park, Jiyoung Lee, Ig-Jae Kim, and Kwanghoon Sohn. Probabilistic representations for video contrastive learning. In *Proceedings of the IEEE/CVF Conference on Computer Vision and Pattern Recognition*, pages 14711–14721, 2022.
- [66] Mandela Patrick, Po-Yao Huang, Yuki Markus Asano, Florian Metze, Alexander G. Hauptmann, João F. Henriques, and Andrea Vedaldi. Support-set bottlenecks for video-text representation learning. In *International Conference on Learning Representations (ICLR)*, 2021. 8
- [67] Leila Pishdad, Ran Zhang, Konstantinos G Derpanis, Allan Jepson, and Afsaneh Fazly. Uncertainty-based cross-modal

- retrieval with probabilistic representations. *arXiv preprint arXiv:2204.09268*, 2022.
- [68] Jesús Andrés Portillo-Quintero, José Carlos Ortiz-Bayliss, and Hugo Terashima-Marín. A straightforward framework for video retrieval using CLIP. In Edgar Roman-Rangel, Ángel Fernando Kuri Morales, José Francisco Martínez Trinidad, Jesús Ariel Carrasco-Ochoa, and José Arturo Olvera-López, editors, *MCPR, Mexico City, Mexico*, volume 12725 of *Lecture Notes in Computer Science*, pages 3–12. Springer, 2021. 8
- [69] Alec Radford, Jong Wook Kim, Chris Hallacy, Aditya Ramesh, Gabriel Goh, Sandhini Agarwal, Girish Sastry, Amanda Askell, Pamela Mishkin, and Jack Clark. Learning transferable visual models from natural language supervision. In *International Conference on Machine Learning*, pages 8748–8763. PMLR, 2021. 1, 2, 4, 8
- [70] A. Radford, J. W. Kim, C. Hallacy, A. Ramesh, G. Goh, S. Agarwal, G. Sastry, A. Askell, P. Mishkin, and J. Clark. Learning transferable visual models from natural language supervision. 2021.
- [71] Anna Rohrbach, Atousa Torabi, Marcus Rohrbach, Niket Tandon, Christopher Pal, Hugo Larochelle, Aaron Courville, and Bernt Schiele. Movie description. *International Journal of Computer Vision*, 123(1):94–120, 2017. 1, 6, 9
- [72] Christof Schuhmann, Richard Vencu, Romain Beaumont, Robert Kaczmarczyk, Clayton Mullis, Aarush Katta, Theo Coombes, Jenia Jitsev, and Aran Komatsuzaki. Laion-400m: Open dataset of clip-filtered 400 million image-text pairs. *arXiv preprint arXiv:2111.02114*, 2021.
- [73] Fangxun Shu, Biaolong Chen, Yue Liao, Shuwen Xiao, Wenyu Sun, Xiaobo Li, Yousong Zhu, Jinqiao Wang, and Si Liu. Masked contrastive pre-training for efficient video-text retrieval. *arXiv preprint arXiv:2212.00986*, 2022. 1, 3
- [74] Yale Song and Mohammad Soleymani. Polysemous visual-semantic embedding for cross-modal retrieval. In *Proceedings of the IEEE/CVF Conference on Computer Vision and Pattern Recognition*, pages 1979–1988, 2019.
- [75] Jennifer J Sun, Jiaping Zhao, Liang-Chieh Chen, Florian Schroff, Hartwig Adam, and Ting Liu. View-invariant probabilistic embedding for human pose. In *European Conference on Computer Vision*, pages 53–70. Springer, 2020.
- [76] Hao Tan, Jie Lei, Thomas Wolf, and Mohit Bansal. Vimpac: Video pre-training via masked token prediction and contrastive learning. *arXiv preprint arXiv:2106.11250*, 2021. 2
- [77] Zhan Tong, Yibing Song, Jue Wang, and Limin Wang. Videomae: Masked autoencoders are data-efficient learners for self-supervised video pre-training. *arXiv preprint arXiv:2203.12602*, 2022. 1, 2
- [78] Aaron van den Oord, Yazhe Li, and Oriol Vinyals. Representation learning with contrastive predictive coding. 2018.
- [79] Limin Wang, Bingkun Huang, Zhiyu Zhao, Zhan Tong, Yinan He, Yi Wang, Yali Wang, and Yu Qiao. Videomae v2: Scaling video masked autoencoders with dual masking. *arXiv preprint arXiv:2303.16727*, 2023. 1
- [80] Qiang Wang, Yanhao Zhang, Yun Zheng, Pan Pan, and Xian-Sheng Hua. Disentangled representation learning for text-video retrieval. *arXiv preprint arXiv:2203.07111*, 2022. 2, 3, 5, 8, 9
- [81] Rui Wang, Dongdong Chen, Zuxuan Wu, Yinpeng Chen, Xiyang Dai, Mengchen Liu, Yu-Gang Jiang, Luwei Zhou, and Lu Yuan. Bevt: Bert pretraining of video transformers. In *Proceedings of the IEEE/CVF Conference on Computer Vision and Pattern Recognition*, pages 14733–14743, 2022.
- [82] Rui Wang, Dongdong Chen, Zuxuan Wu, Yinpeng Chen, Xiyang Dai, Mengchen Liu, Lu Yuan, and Yu-Gang Jiang. Masked video distillation: Rethinking masked feature modeling for self-supervised video representation learning. *arXiv preprint arXiv:2212.04500*, 2022. 3
- [83] Xin Wang, Jiawei Wu, Junkun Chen, Lei Li, Yuan-Fang Wang, and William Yang Wang. Vatex: A large-scale, high-quality multilingual dataset for video-and-language research. In *Proceedings of the IEEE/CVF International Conference on Computer Vision*, pages 4581–4591, 2019.
- [84] Xiaohan Wang, Linchao Zhu, and Yi Yang. T2vlad: global-local sequence alignment for text-video retrieval. In *Proceedings of the IEEE/CVF Conference on Computer Vision and Pattern Recognition*, pages 5079–5088, 2021. 2, 8
- [85] Longhui Wei, Lingxi Xie, Wengang Zhou, Houqiang Li, and Qi Tian. Mvp: Multimodality-guided visual pre-training. In *Computer Vision—ECCV 2022: 17th European Conference, Tel Aviv, Israel, October 23–27, 2022, Proceedings, Part XXX*, pages 337–353. Springer, 2022. 2
- [86] Michael Wray, Hazel Doughty, and Dima Damen. On semantic similarity in video retrieval. In *Proceedings of the IEEE/CVF Conference on Computer Vision and Pattern Recognition*, pages 3650–3660, 2021.
- [87] Peng Wu, Xiangteng He, Mingqian Tang, Yiliang Lv, and Jing Liu. Hanet: Hierarchical alignment networks for video-text retrieval. In *Proceedings of the 29th ACM international conference on Multimedia*, pages 3518–3527, 2021. 1
- [88] Wenhao Wu, Haipeng Luo, Bo Fang, Jingdong Wang, and Wanli Ouyang. Cap4video: What can auxiliary captions do for text-video retrieval? *arXiv preprint arXiv:2301.00184*, 2022.
- [89] Zhenda Xie, Zheng Zhang, Yue Cao, Yutong Lin, Jianmin Bao, Zhuliang Yao, Qi Dai, and Han Hu. Simsim: A simple framework for masked image modeling. In *Proceedings of the IEEE/CVF Conference on Computer Vision and Pattern Recognition*, pages 9653–9663, 2022.
- [90] Jun Xu, Tao Mei, Ting Yao, and Yong Rui. Msr-vtt: A large video description dataset for bridging video and language. In *Proceedings of the IEEE Conference on Computer Vision and Pattern Recognition*, pages 5288–5296, 2016. 1, 6, 7, 8, 9
- [91] Kelvin Xu, Jimmy Ba, Ryan Kiros, Kyunghyun Cho, Aaron Courville, Ruslan Salakhudinov, Rich Zemel, and Yoshua Bengio. Show, attend and tell: Neural image caption generation with visual attention. In *International conference on machine learning*, pages 2048–2057. PMLR, 2015.
- [92] Hongwei Xue, Peng Gao, Hongyang Li, Yu Qiao, Hao Sun, Houqiang Li, and Jiebo Luo. Stare at what you see: Masked

- image modeling without reconstruction. *arXiv preprint arXiv:2211.08887*, 2022.
- [93] Hongwei Xue, Yupan Huang, Bei Liu, Houwen Peng, Jianlong Fu, Houqiang Li, and Jiebo Luo. Probing intermodality: Visual parsing with self-attention for vision-and-language pre-training. *Advances in Neural Information Processing Systems*, 34:4514–4528, 2021. [1](#)
- [94] Hongwei Xue, Yuchong Sun, Bei Liu, Jianlong Fu, Ruihua Song, Houqiang Li, and Jiebo Luo. Clip-vip: Adapting pre-trained image-text model to video-language representation alignment. *arXiv preprint arXiv:2209.06430*, 2022. [1](#), [2](#)
- [95] Jianwei Yang, Yonatan Bisk, and Jianfeng Gao. Taco: Token-aware cascade contrastive learning for video-text alignment. In *Proceedings of the IEEE/CVF International Conference on Computer Vision*, pages 11562–11572, 2021.
- [96] Lewei Yao, Runhui Huang, Lu Hou, Guansong Lu, Minzhe Niu, Hang Xu, Xiaodan Liang, Zhenguo Li, Xin Jiang, and Chunjing Xu. Filip: Fine-grained interactive language-image pre-training. In *International Conference on Learning Representations*, 2021.
- [97] Youngjae Yu, Jongseok Kim, and Gunhee Kim. A joint sequence fusion model for video question answering and retrieval. In *Proceedings of the European Conference on Computer Vision (ECCV)*, pages 471–487, 2018. [1](#), [2](#), [6](#)
- [98] Bowen Zhang, Hexiang Hu, and Fei Sha. Cross-modal and hierarchical modeling of video and text. In *Proceedings of the European Conference on Computer Vision (ECCV)*, pages 374–390, 2018. [6](#)
- [99] Shuai Zhao, Linchao Zhu, Xiaohan Wang, and Yi Yang. Centerclip: Token clustering for efficient text-video retrieval. *arXiv preprint arXiv:2205.00823*, 2022. [1](#), [2](#), [8](#)
- [100] Linchao Zhu and Yi Yang. Actbert: Learning global-local video-text representations. In *Proceedings of the IEEE/CVF conference on computer vision and pattern recognition*, pages 8746–8755, 2020.
- [101] Xiangyang Zhu, Renrui Zhang, Bowei He, Ziyao Zeng, Shanghang Zhang, and Peng Gao. Pointclip v2: Adapting clip for powerful 3d open-world learning. *arXiv preprint arXiv:2211.11682*, 2022. [1](#)